International Journal of Applied Pharmaceutics

ISSN- 0975-7058 Vol 17, Special Issue 1, 2025

Original Article

COMPUTATIONAL STUDY OF COMPOUNDS IN MANGOSTEEN (*GARCINIA MANGOSTANA* L.) AS A CANDIDATE OF LUNG CANCER THERAPY

DIRA HEFNI[1], ZAKKY ANANDA[2], PURNAWAN PONTANA PUTRA[3]*

[1,2]Department of Biology Pharmacy, Faculty of Pharmacy, Universitas Andalas, Padang-25163, Indonesia. [3]Department of Pharmaceutical Chemistry, Faculty of Pharmacy, Universitas Andalas, Padang-25163, Indonesia

***Corresponding author: Purnawan Pontana Putra; *Email: purnawanpp@phar.unand.ac.id**

Received: 05 Oct 2024, Revised and Accepted: 20 Nov 2024

ABSTRACT

Objective: Cancer involves uncontrolled cell growth and spreading to other body parts. Lung cancer is the most common and deadliest cancer worldwide, with treatments often causing significant side effects. This research aims to predict the potential of compounds in mangosteen (*Garcinia mangostana* L.) as a candidate for lung cancer therapy.

Methods: The methods used in this research are network pharmacology analysis using string and cytoscape, molecular docking using deep learning, and molecular dynamics simulations.

Results: Eleven compounds have been identified in *Garcinia mangostana* L., including catechin, gartanin, alpha-mangostin, norathyriol, maclurin, 8-deoxygartanin, beta-mangostin, gamma-mangostin, garcinone A, garcinone B, and garcinone D. Based on ADMET analysis, these compounds exhibit varying degrees of absorption, distribution, metabolism, excretion, and toxicity profiles, which can provide valuable insights into their potential therapeutic applications and safety profiles. It has significant protein targets identified are AURKA, PLK1, CCNA2, and KIF11, with AURKA chosen for molecular docking and molecular dynamics simulations. Molecular docking revealed garcinone D has a binding energy -10.30 kcal/mol and gamma-Mangostin -10.28 kcal/mol had better affinity than the native ligand adenosine-5'-diphosphate -9.00 kcal/mol. Molecular dynamics simulations indicated that garcinone D and gamma-Mangostin were less stable than the native ligand over a 100 ns simulation.

Conclusion: The compounds, including gamma-Mangostin and garcinone D, target the lung cancer-related protein AURKA and are demonstrate to affect key biological pathways such as the cell cycle and motor proteins. Deep learning docking shows that garcinone D and gamma-mangostin exhibit high affinity, while molecular dynamics simulations confirm their stability over 100 ns.

Keywords: Lung cancer, *Garcinia mangostana* L., Network pharmacology, Protein-protein interaction, Deep learning docking, Molecular dynamics simulations

DOI: https://dx.doi.org/10.22159/ijap.2025.v17s1.08 Journal homepage: https://innovareacademics.in/journals/index.php/ijap

INTRODUCTION

Cancer is the leading cause of death worldwide, responsible for nearly 10 million deaths in 2020. With factors like population growth, aging, and changes in lifestyle, the number of cancer cases and related deaths is expected to rise significantly in the coming years [1]. Cancer involves uncontrolled cell growth, tissue invasion, and spreading to other organs [2]. In 2020, the most common cancers were breast, lung, colorectal, prostate, skin, and stomach cancer, with lung cancer being the leading cause of death, caused an estimated 1.8 million deaths (18%) [3].

Despite advances in surgery, chemotherapy, radiotherapy, and targeted drugs, lung cancer mortality rates remain high. Increasing evidence suggests that herbal medicines are a valuable source for prevention or treatment of disease [4]. Indonesia, rich in herbal medicines, has traditionally used these plants for generations. Mangosteen (*Garcinia mangostana* L.), a herbal medicinal in Indonesia's traditional medicine, is known for its anticancer properties [5].

Mangosteen contains xanthones, benzophenones, phenolic, flavonoids, and anthocyanins with xanthones having anticancer properties that induce apoptosis in various cells [6, 7]. Studies show that xanthones in mangosteen skin act as anticancer compounds with anti-proliferative properties that inhibit cancer cell growth [8]. The anticancer mechanism of xanthones involves inducing apoptosis, DNA repair, anti-inflammation, cell cycle modulation, inhibiting angiogenesis, and suppressing cell proliferation. The effectiveness of xanthones and their derivates depends on the functional groups attached to the xanthone framework [9]. However, the synergistic mechanism of multiple compounds in mangosteen against lung cancer remains unclear. This study aims to identify active compounds and their mechanism using a network pharmacology approach. Several studies have shown that mangosteen xanthones, particularly α-mangostin, exhibit anticancer properties by reducing cell viability, inhibiting migration, and inducing apoptosis in lung cancer cell lines such as A549. These effects are mediated through mechanisms like increased ROS generation, altered apoptosis-related protein expression, and cell cycle arrest, with some compounds also demonstrating tumor growth inhibition in animal models [10].

Despite these promising findings, there is still limited understanding of the synergistic mechanisms of multiple bioactive compounds in mangosteen, particularly in the context of lung cancer treatment. Most studies have focused on individual compounds, leaving a gap in understanding how these compounds may work together to enhance anticancer effects. Moreover, the molecular mechanisms that drive the multi-target interactions of these compounds in mangosteen have not been fully elucidated. Network pharmacology approaches study compounds-protein or gene-disease pathways to understand the complex interactions between biological systems, drugs, and diseases, moving beyond the traditional "one drug-one target" principle [11]. This approach reveals the molecular mechanisms and multi-target synergies of plant-based drugs. In this research, network pharmacology was used to investigate the anticancer potential of *Garcinia mangostana* L. compounds, focusing on their molecular mechanism and synergistic effects [12].

The study involved identifying chemical compounds and target proteins from *Garcinia mangostana* L. overlapping these with lung cancer-related genes, performing pathway enrichment analysis, validating interactions through molecular docking, and assessing stability with molecular dynamics simulations. This research aimed to enhance understanding of *Garcinia mangostana* L. compounds and their mechanisms, contributing to the development of safer and

more effective drugs, specifically targeting lung cancer.

MATERIALS AND METHODS

Compounds screening

Collective compounds from *Garcinia mangostana* L. are obtained through the KNApSAcK Family (https://www.knapsackfamily.com/KNApSAcK_Family/) [13] and Dr. Duke's Phytochemical and Ethnobotanical Databases (https://phytochem.nal.usda.gov/phytochem/search) [14]. These compounds are then analyzed for Absorption, Distribution, Metabolism and Excretion (ADME) using SiwssADME (https://www.swissadme.ch/index/php) [15]. Compounds were selected based on criteria including high gastrointestinal absorption, no violation of Lipinski's Rule of Five, and bioavailability ≥ 55% [16].

Identification of potential targets for compounds related with lung cancer

Identify potential targets of the selected compounds using Pharm Mapper (http://www.lilab-ecust.cn/pharmmapper/) [17] with criteria of human proteins with a normalized fit score ≥ 0.8. Further targets were identified using Swiss Target Prediction (http://www.swisstargetprediction.ch/) [18] with a probability criteria of 0.5 and BATMAN (http://bionet.ncpsb.org.cn/batman-tcm/) [19] with a score limit of 80 and an Adjusted P-value of 0.05. Human genes related to lung cancer were annotated from NCBI (https://www.ncbi.nlm.nih.gov/gene/). Target from *Garcinia mangostana* L. were combined with lung cancer-related targets using Venny 2.1 (https://bioinfogp.cnb.csic.es/tools/venny/), with overlapping targets considered as lung cancer-associated targets of *Garcinia mangostana* L. Significant clusters and protein-protein interaction (PPI) data related to lung cancer were obtained from STRING (https://string-db.org/) [20], with interaction parameters set to "Homo sapiens" and a required score of highest confidence (>0.900). PPI data was clustered using CytoCluster in Cytoscape v.3.9.1 (https://cytoscape.org/) with the Cluster ONE algorithm [21], selecting the highest cluster with the lowest p-value as the significant cluster of targets related lung cancer.

Enrichment analysis

Gene Ontology (GO) and KEGG pathway enrichment analyses were performed using DAVID version 6.8 (https://david.ncifcrf.gov/) to explore the functional annotations and pathways associated with the disease targets of *Garcinia mangostana* L. [22]. Significant target clusters were identified based on thresholds set at a minimum count of 10 (with a threshold of 5 for molecular function) and a significance level of $p<0.01$ [23]. The results were visualized using the SRplot platform (http://bioinformatics.com.cn) [24].

Molecular docking

Molecular docking for each selected compound was carried out using GNINA software, which utilizes deep learning techniques [25, 26]. The phytochemical structures were optimized using the molecular mechanics method based on the MMFF94 force field in Avogadro [27]. X-ray crystal structures of the known targets were obtained from the Protein Data Bank (PDB) (https://www.rcsb.org/) with PDB ID: 5ORY (Aurora Kinase A) with organism homo sapiens [28]. During the preparation step, water molecules were removed to obtain rigid protein structures for docking. The docking protocol involved redocking the original ligand with the protein complex to validate the method, ensuring that the RMSD value confirmed accuracy. The binding similarity between the native ligand and test compounds was assessed by analyzing amino acid interactions, CNN pose scores, and binding energies. Protein-ligand interactions were visualized and prepared using BIOVIA Discovery Studio version 2024.

Molecular dynamics simulations

Protein preparation was performed using pdb2gmx in GROMACS. The protein structure was processed to generate a topology file using the CHARMM36 force field [29]. The ligand topology was parameterized with ACPYPE utilizing the General AMBER Force Field (GAFF2) [30]. The TIP3P water model was employed for solvation. Topology and parameter files were created to build a molecular system by placing ligands in the TIP3P water box, followed by solvation and adding NaCl ions to neutralize the system according to physiological conditions. The system then underwent energy minimization to eliminate atomic clashes, followed by temperature and pressure equilibration to achieve a stable state. The equilibration process involved the Canonical NVT Ensemble (constant volume and temperature) followed by the production simulation using the NPT Ensemble (constant pressure and temperature) at 310 K [31, 32]. The molecular dynamics production simulation was conducted using GROMACS 2024.1 software for a total duration of 100 ns.

RESULTS

Compounds of *Garcinia mangostana* L.

The identification of compounds from Garcinia mangostana L. was conducted using KNApSAcK and Dr. Duke's Phytochemical and Ethnobotanical Databases, which led to the identification of 13 compounds. Out of these, 11 compounds were selected for molecular docking based on their favorable ADMET data, particularly their high gastrointestinal (GI) absrobtion, a high GI absorption means that the selected compounds are more likely to be effectively absorbed when administered orally, making them viable therapeutic candidates for oral drug formulations [33]. These selected compounds include Catechin, Gartanin, alpha-Mangostin, Norathyriol, Maclurin, 8-deoxygartanin, beta-Mangostin, gamma-Mangostin, Garcinone A, Garcinone B, and Garcinone D (table 1).

Potential targets for compounds related with lung cancer

Subsequently, protein targets were identified for each compound, yielding 162 unique targets. A total 4,213 lung cancer targets were sourced from NCBI, revealing 92 shared targets between *Garcinia mangostana* L. compounds targets and lung cancer target (fig. 1). This overlap indicates potential targets of *Garcinia mangostana* L. for combating lung cancer.

Table 1: ADME and lipinski's rule screening of *Garcinia mangostana* L. compuounds

Compounds	Chemical formula	Molecular weight (≤500) (g/mol)	MLOGP (≤4,15) (log $P_{o/w}$)	Num. H-bond acceptors (≤10)	Num. H-bond donors (≤5)	GI absorption	Bioavailability
Catechin	$C_{15}H_{14}O_6$	290.27	0.24	6	5	High	55%
Gartanin	$C_{23}H_{24}O_6$	396.43	1.98	6	4	High	55%
alpha-Mangostin	$C_{24}H_{26}O_6$	410.46	2.19	6	3	High	55%
Norathyriol	$C_{13}H_8O_6$	260.20	-0.24	6	4	High	55%
Maclurin	$C_{13}H_{10}O_6$	262.21	0.04	6	5	High	55%
8-deoxygartanin	$C_{23}H_{24}O_5$	380.43	2.52	5	3	High	55%
beta-Mangostin	$C_{25}H_{28}O_6$	424.49	2.40	6	2	High	55%
gamma-Mangostin	$C_{23}H_{24}O_6$	396.43	1.98	6	4	High	55%
Garcinone A	$C_{23}H_{24}O_5$	380.43	2.52	5	3	High	55%
Garcinone B	$C_{23}H_{22}O_6$	394.42	1.98	6	3	High	55%
Garcinone C	$C_{23}H_{26}O_7$	414.45	1.25	7	5	Low	55%
Garcinone D	$C_{24}H_{28}O_7$	428.47	1.46	7	4	High	55%
Garcinone E	$C_{28}H_{32}O_6$	464.55	2.93	6	4	Low	55%

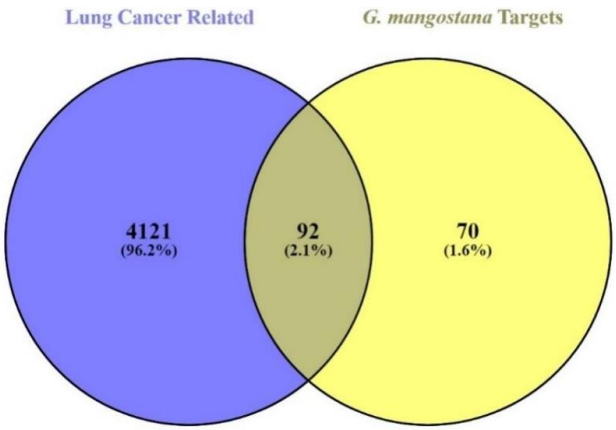

Fig. 1: Venn diagram of compounds targets of *Garcinia mangostana* L. and lung cancer targets

A PPI network was then constructed using Cytoscape software to identify interactions among various protein targets within a complex disease context. The resulting PPI network comprises 3,459 nodes and 15,294 interaction paths. This software also helps explore the significant of potential targets in the PPI network and identify the main clusters using Cluster ONE algorithm a total of 97 clusters were identified, with clusters 12, 16, and 20 having the lowest p-value. Cluster 12 was selected for further analysis as it contained several targets of *Garcinia mangostana* L. compounds.

This cluster has 56 nodes and 685 interactions with a density of 0.4448. The protein contained in this cluster are CDK1, CCNA2, CCNB1, CDC20, PLK1, CCNB2, KIF11, AURKB, KIF20A, DLGAP5, UBE2C, CDCA8, TOP2A, KIF2C, BIRC5, NUF2, AURKA, NUSAP1, TPX2, MELK, ASPM, MAD2L1, TTK, CEP55, CENPE, NDC80, HJURP, NCAPG, KIF4A, RRM2, KIF23, PBK, NEK2, MKI67, FOXM1, ZWINT, ESPL1, FZR1, ANAPC10, KIF15, CDCA3, PTTG1, RACGAP1, CDCA5, KIF14, SPAG5, KIF18A, ECT2, PCLAF, SKA1, KIFC1, NCAPH, TRIP13, RCC2, SHCBP1, and KNTC1 (fig. 2).

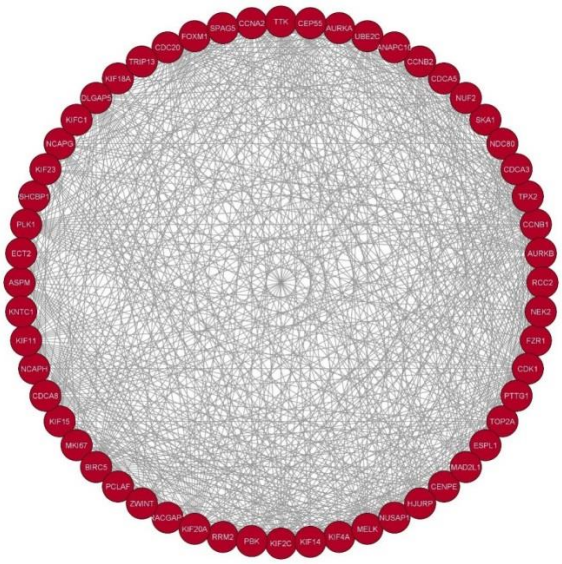

Fig. 2: Significant clusters of lung cancer-related targets using cytoscape

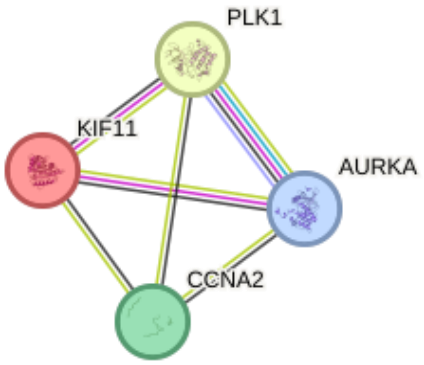

Fig. 3: PPI targets *Garcinia mangostana* L. associated with lung cancer from significant clusters

In this cluster, the targets AURKA, PLK1, CCNA2, and KIF11 were identified as proteins in the significant cluster and were directly targeted by *Garcinia mangostana* L. compounds. A PPI network for these four targets revealed that AURKA (Aurora Kinase A) is the most significant target due to its numerous interactions with other lung cancer-associated proteins (fig. 3).

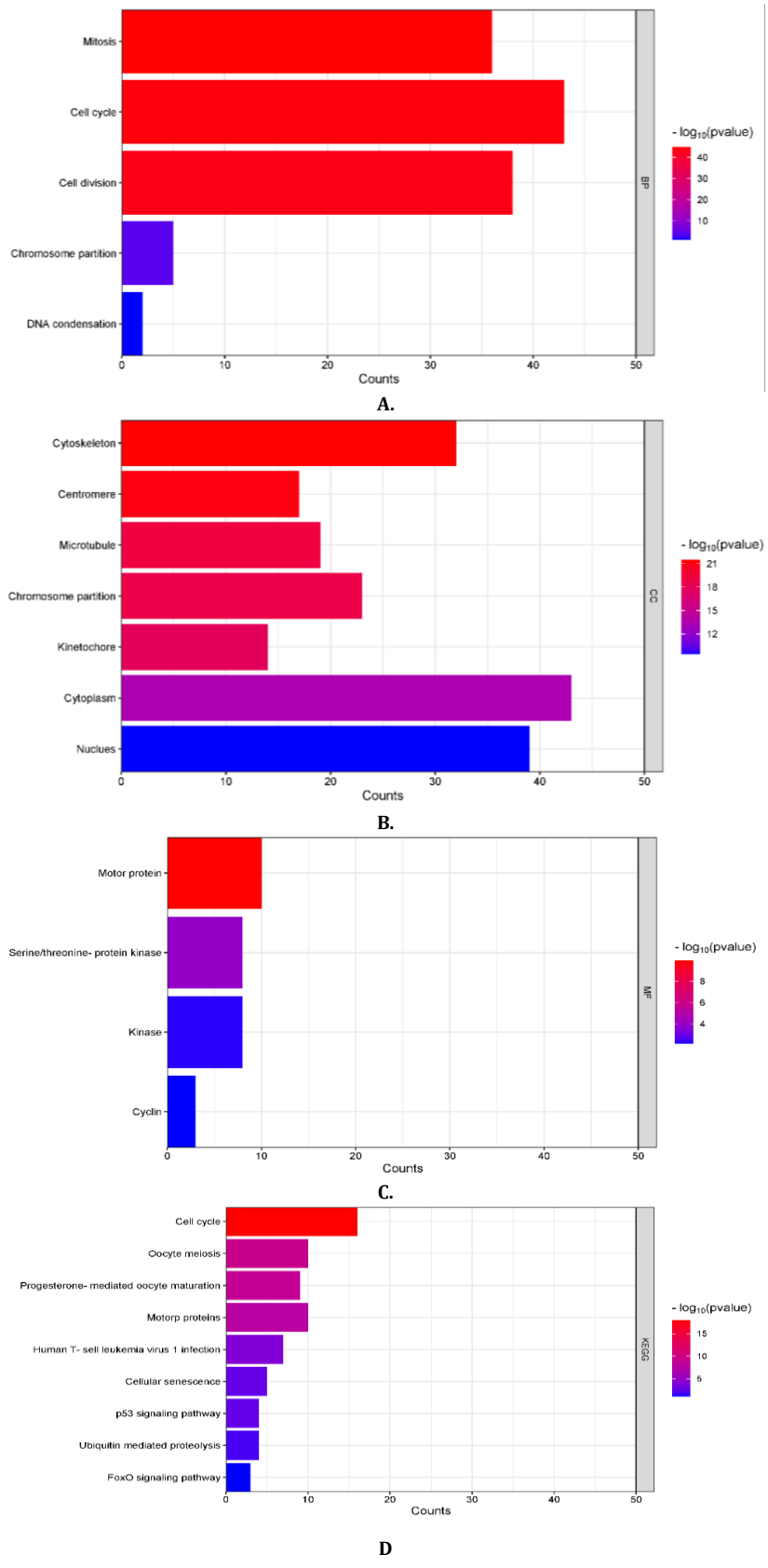

Fig. 4: Enrichment analysis of 56 lung cancer protein targets from significant clusters includes: A) Biological processes, B) Cellular components, C) Molecular function, and D) KEGG Pathways. This fig. was generated using SRplot (http://bioinformatics.com.cn)

Enrichment analysis

GO and KEGG analyses were performed on 56 lung cancer-related targets identified from significant clusters using DAVID. The GO analysis was categorized into three main groups: biological processes, cellular components, and molecular functions. This is crucial for gaining a deeper understanding of the mechanisms through which *Garcinia mangostana* L. may serve as a therapy for lung cancer (fig. 4).

For biological processes, the five GO enrichment terms identified are mitosis, cell cycle, cell division, chromosome partition, and DNA condensation. The cellular components analysis revealed seven GO enrichment terms. The identified components include the cytoskeleton, centromere, microtubule, chromosome partition, kinetochore, cytoplasm, and nucleus. The molecular function analysis revealed four enriched GO terms: motor protein, serine/threonine-protein kinase, kinase, and cyclin. KEGG analysis highlighted nine pathways: cell cycle, oocyte meiosis, progesterone-mediated oocyte maturation, motor proteins, human T-cell leukemia virus type 1 (HTLV-1) infection, cell senescence, p53 signaling pathway, ubiquitin-mediated proteolysis, and FoxO signaling pathway. Among these, four pathways with a p-value less than 0.0001 were deemed crucial for the anticancer activity of *Garcinia mangostana* L. against lung cancer.

Molecular docking

The protein used in this study is AURKA, which corresponds to a significant cluster identified in the PPI network. The PDB ID selected is 5ORY, with adenosine-5'-diphosphate (ADP) as the native ligand. Before proceeding with the molecular docking analysis, the docking process between the protein and its native ligand was validated by assessing the RMSD value. Docking results are considered valid if the RMSD is below 2Å. In this study, an RMSD of 1.27Å was achieved, confirming the validity of the docking process and enabling further analysis of mangosteen compounds.

In deep learning docking, the key parameters for evaluating the interaction between a compound and its target protein are affinity and CNN pose score. The affinity value indicates the strength of the binding interaction, while the CNN pose score measures how accurately the ligand binds at the target protein's binding site, with a score closer to 1 indicating higher accuracy (table 2). These parameters show that gamma-Mangostin (-10.28 kcal/mol) and garcinone D (-10.30 kcal/mol) have the best affinity values compared to the native ligand ADP (-9.00 kcal/mol). Additionally, the CNN pose score of these two compounds are close to 1, suggesting accurate predictions of ligand binding at the target protein's binding site.

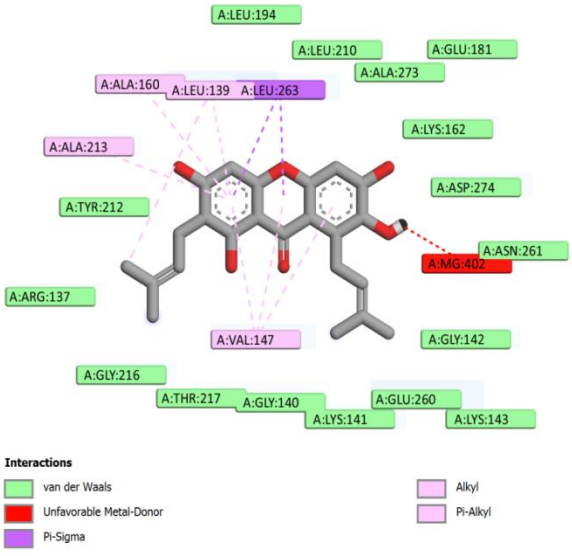

Native Ligand

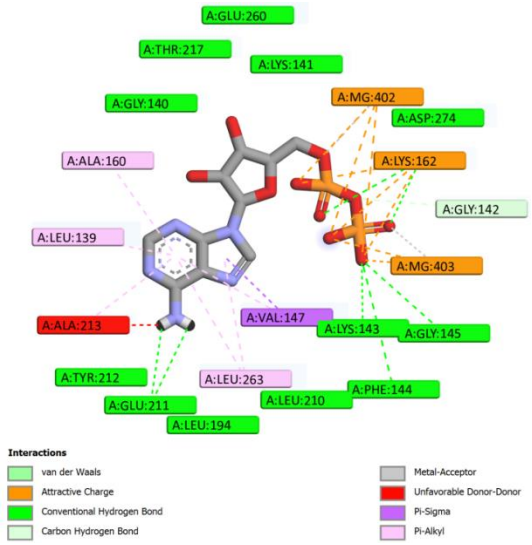

Gamma-Mangostin

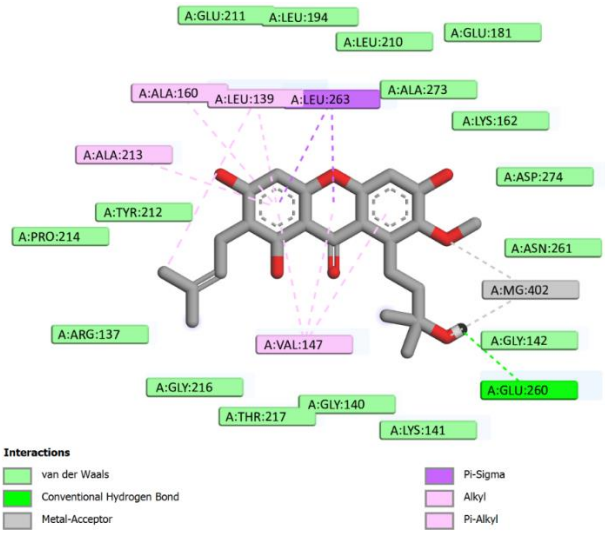

Garcinone D

Fig. 5: The interaction between gamma-Mangostin and Garcinone D showed that these two compounds have the lowest affinity

Table 2: The molecular docking results of compounds from *Garcinia mangostana* L. against aurora kinase a

Compounds	Affinity (kal/mol)	CNN pose score	Hydrogen interaction	Hydrophobic interaction
Native ligand	-9.00	0.9545	Glu 211, Lys 143, Phe 144, Gly 145, Gly 142	Val 147 (Pi-Sigma), Ala 160; Leu 139; Leu 263 (Pi-Alkyl)
Catechin	-9.20	0.8900	Ala 213, Lys 162, Glu 211	Leu 263 (Pi-Sigma), Leu 139; Ala 160; Val 147 (Pi-Alkyl)
Gartanin	-10.00	0.5185	-	Gly 140; Leu 139 (Pi-Sigma), Val 147; Ala 273; Tyr 219; Ala 213; Ala 160; Leu 263; Arg 220 (Pi-Alkyl dan Alkyl)
Alpha-Mangostin	-9.81	0.7338	Leu 139, Gly 140	Leu 263; Val 147 (Pi-Sigma), Tyr 212; Ala 160 (Pi-Alkyl dan Alkyl)
Norathyriol	-8.32	0.8604	Ala 213	Leu 263; Leu 139 (Pi-Sigma), Val 147 (Pi-Alkyl)
Maclurin	-7.15	0.7093	Ala 213, Glu 211, Glu 260	Leu 263 (Pi-Sigma), Ala 160; Leu 139; Val 147 (Pi-Alkyl)
8-deoxygartanin	-9.27	0.6934	-	Leu 263; Leu 139 (Pi-Sigma), Val 147; Lys 162; Ala 273; Leu 194; Leu 210 (Pi-Alkyl dan Alkyl)
Beta-Mangostin	-9.04	0.6007	Asp 274, Gly 140, Gly 142, Glu 211, Glu 260	Tyr 219, Val 147, Leu 263, Leu 139, Leu 194, Ala 160, Tyr 212, Ala 213 (Pi-Alkyl dan Alkyl)
Gamma-Mangostin	-10.28	0.8094	-	Leu 263 (Pi-Sigma), Ala 213; Ala 160; Leu 139; Val 147 (Pi-Alkyl dan Alkyl)
Garcinone A	-9.51	0.7777	Arg 137, Ala 213	Leu 139 (Pi-Sigma), Leu 263; Leu 210; Val 147; Ala 273; Leu 194 (Pi-Alkyl dan Alkyl)
Garcinone B	-9.98	0.6582	Arg 137, Glu 211	Leu 263 (Pi-Sigma), Ala 160; Val 147; Ala 213 (Pi-Alkyl)
Garcinone D	-10.30	0.8014	Glu 260	Leu 263 (Pi-Sigma), Ala 213; Ala 160; Leu 139; Val 147 (Pi-Alkyl dan Alkyl)

Molecular dynamics simulations

The molecular dynamics simulations were conducted based on the optimal molecular docking results, which identified garcinone D and gamma-Mangostin from Garcinia mangostana L. as having the lowest binding affinities with the AURKA target. Following the simulations, analyses of RMSD and RMSF were performed to evaluate the stability and flexibility of the compound-target interactions.

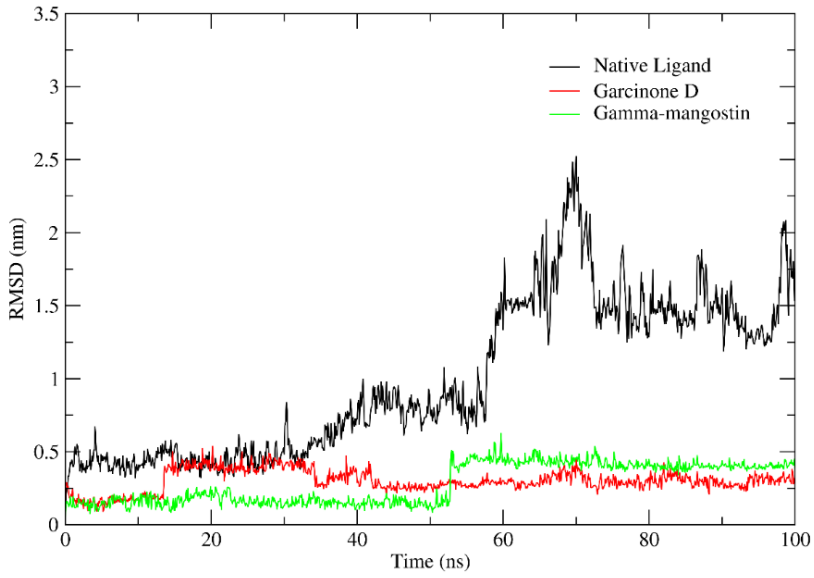

Fig. 6: RMSD graph of native ligands, Garcinone D, and gamma-Mangostin depicts structural stability of Aurora-A kinase over a 100 ns simulation period

The RMSD plot illustrates in fig. 6 was the structural stability of a protein over a 100 ns simulation period when bound to different ligands, revealing that the native ligand (black line) induces greater structural fluctuations and instability, as evidenced by its significantly higher RMSD values compared to the other ligands. This data indicates that while the native ligand initially maintains a stable binding conformation within the first 30 ns of the simulation, its stability is disrupted in the later stages. The spike in RMSD values from 40 ns to 65 ns suggests a significant conformational change or loss of stable interaction between the ligand and the protein. This instability is marked by the peak at 65 ns, where the RMSD reaches its highest value of 2.5 nm, indicating a substantial deviation from its original binding pose. Although there is a partial recovery, with RMSD values decreasing after 65 ns, the ligand does not return to its initial stability, instead showing persistent fluctuations between 1.5 nm and 2.0 nm up to 100 ns. These ongoing fluctuations suggest that the ligands binding remains unstable in the later phase, which could imply weaker interactions or a tendency for the ligand to adopt multiple conformations within the binding site. Understanding these fluctuations is critical, as they can influence the binding efficacy and overall biological activity of the ligand in the context of its interaction with the protein. In contrast, both Garcinone D (red line) and gamma-Mangostin (green line) exhibit relatively low and stable RMSD values with is in the range of 0.25-0.3 nm, suggesting enhanced protein stability, with Garcinone D displaying slightly more flexibility than gamma-mangostin, which shows the least RMSD fluctuations, indicating that it may induce the most favorable binding interactions and stabilize the protein structure more effectively.

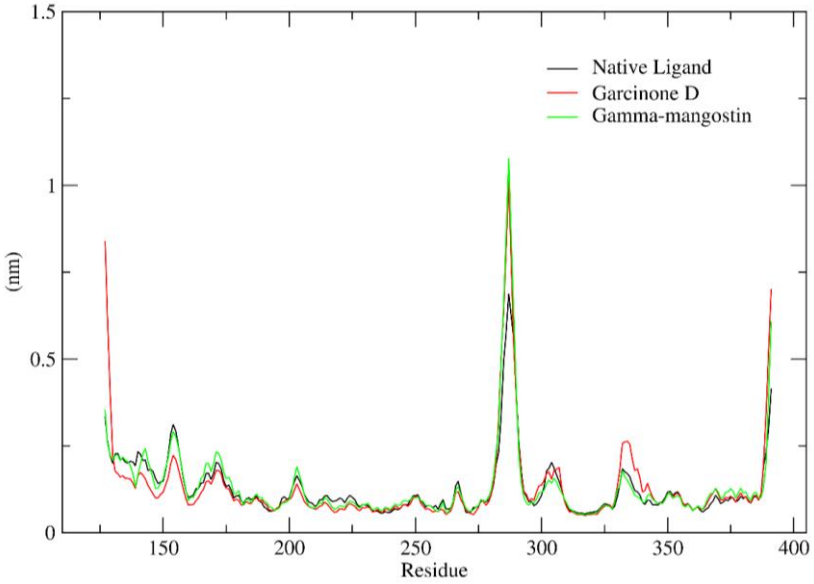

Fig. 7: RMSF graph of the native ligands, Garcinone D and gamma-mangostin depicts overall structural stability of aurora-A kinase

The RMSF plot indicates that while the protein's overall structural stability remains relatively consistent when bound to the native ligand, Garcinone D, and gamma-Mangostin, significant peaks observed around residue 300 reveal a region of high flexibility common to all ligands, with Garcinone D showing slightly increased fluctuations at the sequence's edges (residues below 150 and above 350), suggesting that although the ligands have a similar impact on the protein's general conformation, Garcinone D may induce localized changes in protein dynamics that could influence its functional properties (fig. 7). The RMSF (Root mean Square Fluctuation) results reveal differences in the flexibility of amino acid residue Tyrosine 287 when comparing the native ligand, Garcinone D, and gamma-Mangostin. For the native ligand, residue 287 exhibits an RMSF value of 0.6884 nm, indicating relatively lower flexibility. In contrast, Garcinone D at the same residue shows a higher fluctuation with an RMSF value of 1.0141 nm, while gamma-Mangostin demonstrates the greatest flexibility at residue 287, with an RMSF value of 1.0773 nm.

DISCUSSION

Potential targets of Garcinia mangostana for lung cancer were grouped using the Cluster ONE algorithm, suggesting that proteins within the same cluster are likely to work together or be involved in related biological processes [34]. This clustering helps identify network groups with higher significance, suggesting that proteins with more interactions are more likely to influence lung cancer development [35]. The key protein identified in this study is AURKA. Data from The Cancer Genome Atlas (TCGA) database reveals that 87.9% (29 out of 33) of cancer types exhibit high levels of AURKA expression. In nearly all tumor tissues across 33 cancer types, AURKA expression levels are elevated compared to adjacent normal tissues. Elevated AURKA levels can promote tumorigenesis by enhancing proliferation, inducing genomic and chromosomal instability, exerting antiapoptotic effects, and facilitating epithelial-mesenchymal transition. High AURKA levels can also bypass spindle checkpoint activation caused by abnormal spindle formation, leading to cellular aneuploidy. This uncontrolled cell cycle progression results in the accumulation of abnormal or damaged cells, contributing to malignant transformation [36].

AURKA are important KRAS targets in lung cancer and its inhibition is a novel approach for KRAS-induced lung cancer therapy. Using three different cell-based models, oncogenic KRAS positively regulates the expression of AURKA likely by regulating AURKA transcription or mRNA stability [37]. Furthermore, AURKA can influence drug response in lung cancer treatment. It plays a crucial role in developing resistance to Epidermal Growth Factor Receptor (EGFR) inhibitors in EGFR-mutated adenocarcinoma lung cancer {Formatting Citation}. AURKA activation, driven by the coactivator TPX2 in response to chronic EGFR inhibition, enables cancer cells to survive and proliferate, leading to therapeutic resistance [38]. Inhibition of AURKA with Aurora kinase inhibitors can trigger adaptive survival mechanisms and inhibit apoptosis, potentially prolonging the survival of cancer cells and worsening patient prognosis. Thus, AURKA is a key regulator in the development of resistance to cancer therapy, particularly in lung cancer. Targeting AURKA may effectively prevent resistance and enhance the efficacy of cancer treatments [39].

In deep learning docking, the garcinone D compound demonstrated the best affinity with a score of -10.30 kcal/mol and strong interactions with several amino acids: Glu260, Leu263, Ala213, Ala160, Leu139, and Val147. It also had a CNN pose score of 0.8014. Similarly, the gamma-Mangostin compound showed good affinity, scoring-10.28 kcal/mol and interacting with amino acids Leu263, Ala213, Ala160, Leu139, and Val147, with a CNN pose score of 0.8094 (table 2). Ligand-receptor interactions aim to achieve the lowest energy state, resulting in a stable molecule. These interactions include electrostatic interactions, hydrophobic interactions, and hydrogen bonds, with amino acid residues playing a crucial role in ligand binding at the protein binding sites. Garcinone D and gamma-Mangostin compounds showed the highest affinity towards protein targets, with values of -10.30 kcal/mol and-10.28 kcal/mol respectively, which indicated a strong interaction. However, the CNN pose scores of both are slightly lower (0.8014 and 0.8094) than those of the native ligand (0.9545), indicating that the orientation of these compounds is not as optimal as the pose of the native ligand. This CNN pose score indicates how close the compound's orientation is to the original ligand, where the closer it is to 1, the more similar it is to the original pose. Catechin (0.8900) and Norathyriol (0.8604) approach the orientation of the native ligand, but their affinity is lower. Meanwhile, Gartanin despite having good affinity (-10.00 kcal/mol), has the lowest CNN pose score (0.5185). This protein cluster in fig. 2, made up of 56 nodes and 685 interactions with a density of 0.4448, plays a key role in cell division, helping to regulate important processes like the cell cycle and mitosis.

Several amino acids are similarly involved in the interactions between the native ligand ADP, garcinone D, and gamma-Mangostin with the 5ORY protein, specifically Val147, Ala160, Leu 139, and Leu293 (fig. 5). ADP binds specifically to the active site region of the Aurora-A kinase protein, a critical area where catalytic interactions occur. This implies that compounds derived from *Garcinia*

mangostana L., such as garcinone D or gamma-mangostin, are also expected to target the same active site region for their potential inhibitory effects. Both gamma-mangostin and garcinone D demonstrate hydrophobic interactions with residues within the ADP binding site, specifically Leu139, Val147, Ala160, and Leu263, which are critical for ADP's binding affinity and activity at the active site. Notably, garcinone D also forms a hydrogen bond with Glu260, mirroring a key interaction of ADP in the active site. This additional hydrogen bonding indicates that garcinone D better replicates ADP's interaction profile, emphasizing its potential as a mimic of the native ligand within the active site region.

Central players like CDK1, Cyclins (such as CCNA2 and CCNB1), Aurora kinases (AURKA and AURKB), and kinesins (members of the KIF family) are crucial for guiding cells through each step of division, from preparing to split to correctly distributing genetic material. Proteins like CDC20 and PLK1 help make sure cells only move forward when everything's properly aligned, while others, like MAD2L1 and the APC/C components (ANAPC10, FZR1), act as checkpoints to catch any mistakes before they become problems. Proteins involved in DNA repair and replication, like TOP2A and RRM2, play a vital role in safeguarding genetic information, while markers like MKI67 and FOXM1 are linked to cell growth. The tightly-knit connections within this cluster suggest that these proteins work closely together to keep cell division precise and controlled, which is essential to preventing errors that could lead to diseases like cancer. Understanding how this network functions opens up possibilities for developing therapies that target these proteins to stop cells from dividing uncontrollably.

In silico drug discovery and design is often used to increase efficiency [40], but traditional molecular docking methods do not account for protein flexibility. To address this, molecular dynamics simulations are performed to gain clearer insights into protein-ligand interactions under flexible conditions [41]. The goal of molecular dynamics is to observe the stability of these interactions in environments that closely mimic human physiological conditions over time. The molecular dynamics process begins with energy minimization to reduce atom clashes and contacts caused by the addition or removal of hydrogen atoms. This step systematically adjusts atom positions to minimize molecular stress [42]. Following minimization, the equilibration process takes place, allowing the system to reach the desired temperature and achieve thermodynamic equilibrium. During this phase, temperature, volume, pressure, and energy stabilize, ensuring a more accurate subsequent analysis [43].

After the production process, RMSD and RMSF graphic analyses are conducted. RMSD (Root mean Square Deviation) measures structural similarity between molecular conformations, evaluating changes in protein molecular dynamics and the conformational stability of the protein-ligand complex over time [44]. The results of the molecular dynamics simulations indicate that the two compounds, Garcinone D and gamma-Mangostin, are relatively more stable compared to the native ligand. RMSF (Root mean Square Fluctuation), on the other hand, calculates the fluctuation of amino acid residues during the simulation. The RMSF per residue is plotted against the residue number, highlighting which amino acids contribute most to molecular movement and folding [45]. Peaks in the RMSF graph indicate residues with the largest oscillations, where higher RMSF values suggest high flexibility and potentially unstable interactions due to frequent positional changes [46]. The RMSD and RMSF plots reveal differences in the structural stability and flexibility of the proteins when bound to native ligands, Garcinone D, and gamma-Mangostin during 100 ns simulations. The native ligand shows larger structural fluctuations, especially after 30 ns, with an RMSD peak at 65 ns (2.5 nm), indicating interaction instability in the late stages of the simulation. In contrast, Garcinone D and gamma-mangostin showed lower RMSD values (0.25-0.3 nm), indicating better stability, with gamma-mangostin showing the least fluctuations. In the RMSF plot, residue Tyrosine 287 shows higher flexibility when bound to Garcinone D (RMSF 1.0141 nm) and gamma-mangostin (1.0773 nm) than the native ligand (0.6884 nm), indicating that these two ligands increase the local flexibility of the protein. These differences suggest that while Garcinone D and gamma-Mangostin increase the global stability of proteins, they also affect the flexibility of certain residues, which can influence overall protein dynamics and function. These differences suggest that both Garcinone D and gamma-Mangostin induce greater movement or flexibility at this specific amino acid compared to the native ligand, which may influence the protein's overall dynamics and stability. This fluctuation can be concluded to be meaningless because the fluctuating residue is not the active site of the protein. Based on RMSD and RMSF analyses, the Garcinone D and gamma-Mangostin produced the best molecular dynamics results. The RMSD value of the native ligand was not within the acceptable range, it was lower compared to garcinone D and gamma-Mangostin. Additionally, the RMSF analysis showed that the amino acid residues of the native ligand, garcinone D, and gamma-Mangostin had similar fluctuations and did not fluctuate at the protein binding site.

Network pharmacology allows for the analysis of complex interactions between multiple compounds and their targets. Data can be integrated from various sources, including genomics, proteomics, and metabolomics [47]. By mapping out the interactions between compounds and multiple biological targets, combinations of 11 compounds from *Garcinia mangostana* L. can affect pathway simultaneously. This holistic approach is beneficial for understanding how different compounds can work together synergistically for lung cancer treatment.

CONCLUSION

The multi-compound synergy mechanism of *Garcinia mangostana* L. can be explored through network pharmacology. In this study, 11 compounds meeting the rule of five criteria (catechin, gartanin, alpha-Mangostin, norathyriol, maclurin, 8-deoxygartanin, beta-Mangostin, gamma-Mangostin, garcinone A, garcinone B, and garcinone D) were linked to the significant lung cancer protein AURKA (Aurora Kinase A). Significant proteins are typically associated with biological processes like cell cycle regulation and division. The predicted mechanism of *Garcinia mangostana* L. compounds against lung cancer involves four pathways (cell cycle, oocyte meiosis, progesterone-mediated oocyte maturation, motor proteins), which are likely inhibited by these compounds. Deep learning docking showed that garcinone D (-10.30 kcal/mol) and gamma-Mangostin (-10.28 kcal/mol) had better affinity compared to the native ligand adenosine-5'-diphosphate (-9.00 kcal/mol). However, molecular dynamics simulations indicated that garcinone D and gamma-Mangostin stable during a 100 ns simulation based on RMSD values.

ACKNOWLEDGEMENT

We sincerely appreciate the support, guidance, and financial assistance the Faculty of Pharmacy Universitas Andalas.

FUNDING

This Research was funded by Research Fund for Lecturer Development and DIPA of the Faculty of Pharmacy for the 2021 Fiscal Year with contract Number: 05/UN16.10. D/PJ.01./2021.

AUTHORS CONTRIBUTIONS

Dira Hefni contributed to the study's conceptualization, revised the manuscript, and conducted a comprehensive review. Zakky Ananda performed the network pharmacology analysis, molecular docking, and ADMET analysis, and contributed to manuscript writing. Purnawan Pontana Putra conceptualized the entire study, including the introduction, methods, and discussion sections, conducted molecular dynamics simulations, and wrote the manuscript.

CONFLICT OF INTERESTS

The authors have no known competing interests that could call into question the objectivity of this research.

REFERENCES

1. Singer S. Psychosocial impact of cancer. Recent Results Cancer Res. 2018;210:1-11. doi: 10.1007/978-3-319-64310-6_1, PMID 28924676.

2. DiPiro JT, Yee GC, Posey LM, Haines ST, Nolin TD, Ellingrod VL. Pharmacotherapy: a pathophysiologic approach. McGraw-Hill Education; 2020.
3. Sung H, Ferlay J, Siegel RL, Laversanne M, Soerjomataram I, Jemal A. Global cancer statistics 2020: GLOBOCAN estimates of incidence and mortality worldwide for 36 cancers in 185 countries. CA Cancer J Clin. 2021;71(3):209-49. doi: 10.3322/caac.21660, PMID 33538338.
4. Zhang Q, Liu J, Li R, Zhao R, Zhang M, Wei S. A network pharmacology approach to investigate the anticancer mechanism and potential active ingredients of Rheum palmatum L. against lung cancer via induction of apoptosis. Front Pharmacol. 2020;11:528308. doi: 10.3389/fphar.2020.528308, PMID 33250766.
5. EL-Kenawy AE, Hassan SM, Osman HE. Mangosteen (Garcinia mangostana L.) nonvitamin and nonmineral nutritional supplements. Amsterdam: Elsevier; 2019. p. 313-9. doi: 10.1016/B978-0-12-812491-8.00045-X.
6. Andayani R, Armin F, Mardhiyah A. Determination of the total phenolics and antioxidant activity in the rind extracts of Garcinia mangostana L., Garcinia Cowa Roxb., and garcinia atroviridis griff. Ex T. Anders. Asian J Pharm Clin Res. 2020;13(8):149-52. doi: 10.22159/ajpcr.2020.v13i8.36525.
7. Ovalle Magallanes B, Eugenio Perez D, Pedraza Chaverri J. Medicinal properties of mangosteen (Garcinia mangostana L.): a comprehensive update. Food Chem Toxicol. 2017;109(1):102-22. doi: 10.1016/j.fct.2017.08.021, PMID 28842267.
8. Nauman MC, Johnson JJ. The purple mangosteen (Garcinia mangostana): defining the anticancer potential of selected xanthones. Pharmacol Res. 2022;175:106032. doi: 10.1016/j.phrs.2021.106032, PMID 34896543.
9. Gul S, Aslam K, Pirzada Q, Rauf A, Khalil AA, Semwal P. Xanthones: a class of heterocyclic compounds with anticancer potential. Curr Top Med Chem. 2022;22(23):1930-49. doi: 10.2174/1568026622666220901145002, PMID 36056870.
10. Kalick LS, Khan HA, Maung E, Baez Y, Atkinson AN, Wallace CE. Mangosteen for malignancy prevention and intervention: current evidence, molecular mechanisms, and future perspectives. Pharmacol Res. 2023;188:106630. doi: 10.1016/j.phrs.2022.106630, PMID 36581166.
11. Zhang R, Zhu X, Bai H, Ning K. Network pharmacology databases for traditional Chinese medicine: review and assessment. Front Pharmacol. 2019;10:123. doi: 10.3389/fphar.2019.00123, PMID 30846939.
12. Patil SA, Patil VS, Malgi AP, Hupparage VB, Mallapur SP, Naik RR. Cananga odorata (Ylang-Ylang) modulate pathways involved in cancer: gene set enrichment and network pharmacology approach. Int J Ayurvedic Med. 2023;14(2):453-63. doi: 10.47552/ijam.v14i2.3434.
13. Afendi FM, Okada T, Yamazaki M, Hirai Morita A, Nakamura Y, Nakamura K. KNApSAcK family databases: integrated metabolite-plant species databases for multifaceted plant research. Plant Cell Physiol. 2012;53(2):e1. doi: 10.1093/pcp/pcr165, PMID 22123792.
14. US Department of Agriculture ARS. Dr. Duke's phytochemical and ethnobotanical databases; 2016.
15. Daina A, Michielin O, Zoete V. Swiss ADME: a free web tool to evaluate pharmacokinetics, drug-likeness and medicinal chemistry friendliness of small molecules. Sci Rep. 2017;7:42717. doi: 10.1038/srep42717, PMID 28256516.
16. Benet LZ, Hosey CM, Ursu O, Oprea TI. BDDCS, the rule of 5 and drug ability. Adv Drug Deliv Rev. 2016;101:89-98. doi: 10.1016/j.addr.2016.05.007, PMID 27182629.
17. Wang X, Shen Y, Wang S, Li S, Zhang W, Liu X. Pharm mapper 2017 update: a web server for potential drug target identification with a comprehensive target pharmacophore database. Nucleic Acids Res. 2017;45(W1):W356-60. doi: 10.1093/nar/gkx374, PMID 28472422.
18. Daina A, Michielin O, Zoete V. Swiss target prediction: updated data and new features for efficient prediction of protein targets of small molecules. Nucleic Acids Res. 2019;47(W1):W357-64. doi: 10.1093/nar/gkz382, PMID 31106366.
19. Liu Z, Guo F, Wang Y, Li C, Zhang X, Li H. BATMAN-TCM: a bioinformatics analysis tool for molecular mech ANism of traditional chinese medicine. Batman. Sci Rep. 2016;6(1). doi: 10.1038/srep21146.
20. Szklarczyk D, Gable AL, Nastou KC, Lyon D, Kirsch R, Pyysalo S. The STRING database in 2021: customizable protein-protein networks, and functional characterization of user-uploaded gene/measurement sets. Nucleic Acids Res. 2021;49(D1):D605-12. doi: 10.1093/nar/gkaa1074, PMID 33237311.
21. Shannon P, Markiel A, Ozier O, Baliga NS, Wang JT, Ramage D. Cytoscape: a software environment for integrated models of biomolecular interaction networks. Genome Res. 2003;13(11):2498-504. doi: 10.1101/gr.1239303, PMID 14597658.
22. Jiao X, Sherman BT, Huang DW, Stephens R, Baseler MW, Lane HC. David-WS: a stateful web service to facilitate gene/protein list analysis. Bioinformatics. 2012;28(13):1805-6. doi: 10.1093/bioinformatics/bts251, PMID 22543366.
23. Reimand J, Isserlin R, Voisin V, Kucera M, Tannus Lopes C, Rostamianfar A. Pathway enrichment analysis and visualization of omics data using g: profiler, GSEA, cytoscape and enrichment map. Nat Protoc. 2019;14(2):482-517. doi: 10.1038/s41596-018-0103-9, PMID 30664679.
24. Tang D, Chen M, Huang X, Zhang G, Zeng L, Zhang G. SRplot: a free online platform for data visualization and graphing. PLOS One. 2023;18(11):e0294236. doi: 10.1371/journal.pone.0294236, PMID 37943830.
25. McNutt AT, Francoeur P, Aggarwal R, Masuda T, Meli R, Ragoza M. GNINA 1.0: molecular docking with deep learning. J Cheminform. 2021;13(1):43. doi: 10.1186/s13321-021-00522-2, PMID 34108002.
26. Putra PP, Indradi RB, Yuniarta TA, Hanifa D, Syaban MF, Suharti N. Computational investigation of pluchea indica mechanism targeting peroxisome proliferator-activated receptor gamma. J HerbMed Pharmacol. 2024;13(4):630-9. doi: 10.34172/jhp.2024.52544.
27. Hanwell MD, Curtis DE, Lonie DC, Vandermeersch T, Zurek E, Hutchison GR. Avogadro: an advanced semantic chemical editor, visualization, and analysis platform. J Cheminform. 2012;4(1):17. doi: 10.1186/1758-2946-4-17, PMID 22889332.
28. McIntyre PJ, Collins PM, Vrzal L, Birchall K, Arnold LH, Mpamhanga C. Characterization of three druggable hot-spots in the Aurora-A/TPX2 interaction using biochemical, biophysical, and fragment-based approaches. ACS Chem Biol. 2017;12(11):2906-14. doi: 10.1021/acschembio.7b00537, PMID 29045126.
29. Huang J, Rauscher S, Nawrocki G, Ran T, Feig M, De Groot BL. CHARMM36m: an improved force field for folded and intrinsically disordered proteins. Nat Methods. 2017;14(1):71-3. doi: 10.1038/nmeth.4067, PMID 27819658.
30. Sousa da Silva AW, Vranken WF. Acpype-Ante chamber python parser interface. BMC Res Notes. 2012;5:367. doi: 10.1186/1756-0500-5-367, PMID 22824207.
31. Hussain S, Iqbal A, Hamid S, Putra PP, Ashraf M. Identifying alkaline phosphatase inhibitory potential of cyclooxygenase-2 inhibitors: insights from molecular docking, MD simulations, molecular expression analysis in MCF-7 breast cancer cell line and *in vitro* investigations. Int J Biol Macromol. 2024;277(2):132721. doi: 10.1016/j.ijbiomac.2024.132721, PMID 38815949.
32. Kurniawan R, Taslim NA, Hardinsyah H, Syauki AY, Idris I, Aman AM. Pharmacoinformatics and cellular studies of algal peptides as functional molecules to modulate type-2 diabetes markers. Future Foods. 2024;9. doi: 10.1016/j.fufo.2024.100354.
33. Velez LA, Delgado Y, Ferrer Acosta Y, Suarez Arroyo IJ, Rodriguez P, Perez D. Theoretical prediction of gastrointestinal absorption of phytochemicals. Int J Plant Biol. 2022;13(2):163-79. doi: 10.3390/ijpb13020016.
34. Nepusz T, Yu H, Paccanaro A. Detecting overlapping protein complexes in protein-protein interaction networks. Nat Methods. 2012;9(5):471-2. doi: 10.1038/nmeth.1938, PMID 22426491.
35. Niemira M, Collin F, Szalkowska A, Bielska A, Chwialkowska K, Reszec J. Molecular signature of subtypes of non-small-cell lung cancer by large-scale transcriptional profiling: identification of key modules and genes by weighted gene co-expression

network analysis (WGCNA). Cancers (Basel). 2019;12(1):37. doi: 10.3390/cancers12010037, PMID 31877723.

36. Mou PK, Yang EJ, Shi C, Ren G, Tao S, Shim JS. Aurora kinase a, a synthetic lethal target for precision cancer medicine. Exp Mol Med. 2021;53(5):835-47. doi: 10.1038/s12276-021-00635-6, PMID 34050264.
37. Dos Santos EO, Carneiro-Lobo TC, Aoki MN, Levantini E, Basseres DS. Aurora kinase targeting in lung cancer reduces KRAS-induced transformation. Mol Cancer. 2016;15:12. doi: 10.1186/s12943-016-0494-6, PMID 26842935.
38. Galetta D, Cortes Dericks L. Promising therapy in lung cancer: spotlight on Aurora kinases. Cancers (Basel). 2020;12(11):3371. doi: 10.3390/cancers12113371, PMID 33202573.
39. Shah KN, Bhatt R, Rotow J, Rohrberg J, Olivas V, Wang VE. Aurora kinase a drives the evolution of resistance to third-generation EGFR inhibitors in lung cancer. Nat Med. 2019;25(1):111-8. doi: 10.1038/s41591-018-0264-7, PMID 30478424.
40. Kurian T. In silico screening by molecular docking of heterocyclic compounds with furan or indole nucleus from database for anticancer activity and validation of the method by redocking. Int J Pharm Pharm Sci. 2024;16:42-5. doi: 10.22159/ijpps.2024v16i4.50478.
41. De Vivo M, Masetti M, Bottegoni G, Cavalli A. Role of molecular dynamics and related methods in drug discovery. J Med Chem. 2016;59(9):4035-61. doi: 10.1021/acs.jmedchem.5b01684, PMID 26807648.
42. Santos LH, Ferreira RS, Caffarena ER. Integrating molecular docking and molecular dynamics simulations. Methods Mol Biol. 2019;2053:13-34. doi: 10.1007/978-1-4939-9752-7_2, PMID 31452096.
43. Gerrard JA, Domigan LJ. Protein nanotechnology: protocols, instrumentation, and applications. 3rd ed. Humana Press; 2020.
44. Ghahremanian S, Rashidi MM, Raeisi K, Toghraie D. Molecular dynamics simulation approach for discovering potential inhibitors against SARS-CoV-2: a structural review. J Mol Liq. 2022;354:118901. doi: 10.1016/j.molliq.2022.118901, PMID 35309259.
45. Putra PP, Asnawi A, Hamdayuni F, Arfan ALO, Aman LO. Pharmacoinformatics analysis of Morus macroura for drug discovery and development. Int J Appl Pharm. 2024;16:111-7. doi: 10.22159/ijap.2024.v16s1.26.
46. Tripathi N, Goel B, Bhardwaj N, Sahu B, Kumar H, Jain SK. Virtual screening and molecular simulation study of natural products database for lead identification of novel coronavirus main protease inhibitors. J Biomol Struct Dyn. 2022;40(8):3655-67. doi: 10.1080/07391102.2020.1848630, PMID 33213294.
47. Noor F, Asif M, Ashfaq UA, Qasim M, Tahir Ul Qamar M. Machine learning for synergistic network pharmacology: a comprehensive overview. Brief Bioinform. 2023;24(3):bbad120. doi: 10.1093/bib/bbad120, PMID 37031957.